Effect of nonmagnetic dilution in the honeycomb-lattice iridates Na2IrO3 and Li2IrO3

S. Manni, Yoshifumi Tokiwa, Philipp Gegenwart

Effect of nonmagnetic dilution in the honeycomb-lattice iridates Na_2IrO_3 and Li_2IrO_3

S. Manni,[1] Y. Tokiwa,[1,*] and P. Gegenwart[1,2]

[1]*I. Physikalisches Institut, Georg-August-Universität Göttingen, 37077 Göttingen, Germany*
[2]*Experimentalphysik VI, Center for Electronic Correlations and Magnetism, Augsburg University, 86159 Augsburg, Germany*

We have synthesized single crystals of $Na_2(Ir_{1-x}Ti_x)O_3$ and polycrystals of $Li_2(Ir_{1-x}Ti_x)O_3$ and studied the effect of magnetic depletion on the magnetic properties by measurements of the magnetic susceptibility, specific heat, and magnetocaloric effect at temperatures down to 0.1 K. In both systems, the nonmagnetic substitution rapidly changes the magnetically ordered ground state into a spin glass, indicating strong frustration. While for the Li system the Weiss temperature Θ_W remains unchanged up to $x = 0.55$, a strong decrease $|\Theta_W|$ is found for the Na system. This suggests that only for the former system magnetic exchange beyond nearest neighbors is dominating. This is also corroborated by the observation of a smeared quantum phase transition in $Li_2(Ir_{1-x}Ti_x)O_3$ near $x = 0.5$, i.e., much beyond the site percolation threshold of the honeycomb lattice.

Iridates have attracted considerable interest in the last few years due to their potential to host novel electronic and magnetic phases mediated by the combination of strong spin-orbit (SO) coupling and electronic correlations [1–5]. Layered honeycomb lattice iridates A_2IrO_3 ($A = $ Na,Li) are intensively investigated because they have been proposed as candidate materials for the realization of the highly frustrated Kitaev interaction [6] as well as correlated topological insulator phases [7,8].

Both Na_2IrO_3 and Li_2IrO_3 are electrically insulating with fluctuating $S_{eff} = 1/2$ moments above an antiferromagnetic (AF) ordering around 15 K [9,10]. Their electronic structure is discussed either within $J_{eff} = 1/2$ SO Mott insulator [11] or quasimolecular orbital (QMO) scenarios [12,13], where the upper half-filled $J_{eff} = 1/2$ or QMO doublet, respectively, causes magnetism. At present, the correct effective Hamiltonians for the description of magnetic exchange in the two systems are not settled. Na_2IrO_3 displays an AF Weiss temperature of -120 K [9] and zigzag ground state [14]. Within the next-neighbor Heisenberg-Kitaev (HK) model this would require ferromagnetic (FM) Heisenberg and AF Kitaev couplings [15], which, however, seems incompatible with *ab initio* DFT calculations [13]. Significant further neighbor exchange in a J_1-J_2-J_3 Heisenberg model has been concluded from the analysis of the measured magnon dispersion in Na_2IrO_3 [14]. On the other hand, it has been pointed out recently that trigonal distortions present in the system lead to an anisotropic contribution to the next-neighbor exchange, which together with a FM Kitaev interaction can reproduce the experimental results [16].

Isostructural honeycomb Li_2IrO_3 displays a significantly smaller AF Weiss temperature (-30 K) compared to Na_2IrO_3 [10]. Recent neutron scattering has detected a magnetic Bragg peak within the first Brillouin zone, indicating incommensurate spiral ordering [17]. Due to the much reduced atomic size of Li, its substitution for Na in $(Na_{1-x}Li_x)_2IrO_3$ revealed that up to $x = 0.25$ preferentially only the Na sites in the honeycomb plane are occupied by Li and further doping results in chemical phase segregation [18]. Magnetic properties of Na_2IrO_3 and Li_2IrO_3 thus differ significantly [18,19]. Due to the smaller Ir-Ir distances in the honeycomb planes in Li_2IrO_3, one may expect enhanced further neighbor exchange in this system.

Introduction of random vacancies to frustrated magnets induces spin-glass behavior. For striped phases of the HK model, it has been shown that the vacancies locally select specific stripe orientations [20]. It has recently been proposed that systematic depletion of the Ir spins by a nonmagnetic ion could provide important new insights on the magnetic exchange in these materials. Andrade and Vojta have shown by classical Monte Carlo simulations that the spin-glass freezing temperatures for depleted next neighbor HK and J_1-J_2-J_3 Heisenberg magnets behave significantly different when the doping concentrations exceed the site percolation threshold $x_p = 0.303$ [21]. While in the former case the freezing temperature rapidly drops to zero, spin-glass ordering has a tail and can largely extend into the regime $x > x_p$ for substantial further neighbor magnetic exchange.

We have studied $Na_2(Ir_{1-x}Ti_x)O_3$ and $Li_2(Ir_{1-x}Ti_x)O_3$ where magnetic Ir^{4+} is randomly substituted by nonmagnetic Ti^{4+}. In contrast to the Na system, for the Li system, the AF Weiss temperature remains almost unchanged and spin-glass freezing is found up to $x = 0.55$, highlighting the importance of further neighbor exchange in the latter system.

We have chosen nonmagnetic Ti as substituent because Ti^{4+} and Ir^{4+} have a very similar ionic radius. In compounds where Ir and Ti occupy different sites this causes a severe problem due to site exchange [22], while in our case, it assures a good statistical mixing of Ir and Ti in the diluted systems. $Na_2(Ir_{1-x}Ti_x)O_3$ single crystals were grown using a similar method as for Na_2IrO_3, by prereacting Na_2CO_3, Ir metal powder and TiO_2 powder at 750 °C to 900 °C. The subsequent crystal growth was done with 10% extra IrO_2 in between 1030–1050 °C. Unfortunately, this method only worked for compositions $x \leqslant 0.3$. At larger x, only a solid melt of Na_2TiO_3 was obtained and no $Na_2(Ir_{1-x}Ti_x)O_3$ crystals were formed. Na_2TiO_3 has a very low melting point of 180 °C, which causes this problem for $x > 0.3$. Since

---

*Present address: Research Center for Low Temperature and Materials Science, Kyoto University, Kyoto 606-8501, Japan.

the chemistry and crystal structure of Na_2TiO_3 differs from Na_2IrO_3, attempts to synthesize single-phase $Na_2(Ir_{1-x}Ti_x)O_3$ polycrystals for $x > 0.3$ have failed.

For $Li_2(Ir_{1-x}Ti_x)O_3$, we have prepared well ordered single phase polycrystals up to $x = 0.55$ by solid state reaction. At higher doping, $Li_2(Ir_{1-x}Ti_x)O_3$ polycrystals become disordered probably due to a site exchange between Li and Ti. For polycrystal synthesis Li_2CO_3, Ir metal powder and TiO_2 were mixed and reacted in the open furnace at 700–1000 °C in 100 °C steps after repetitive grinding and pelletizing after each step. Phase purity and structural ordering were verified from powder x-ray diffraction (XRD). The detailed structural analysis of $Li_2(Ir_{1-x}Ti_x)O_3$ by powder XRD (see Ref. [24]) shows that the changes in the lattice parameters are within 1% as expected because the ionic radius of Ti^{4+} and Ir^{4+} are similar. For the elemental quantification of the Ir and Ti content, several spots on various pieces of each batch have been studied by the energy dispersive x-ray (EDX) method. Throughout this Rapid Communication, x always denotes the actual Ti concentration. Magnetization, ac susceptibility, and specific heat measurements were conducted in the Quantum Design MPMS and PPMS. Thermodynamic measurements below 0.4 K were performed in a dilution refrigerator [23].

Magnetization measurements on $Na_2(Ir_{1-x}Ti_x)O_3$ single crystals show that for all investigated x the magnetic susceptibility $\chi = M/H$ follows the Curie-Weiss (CW) behavior $\chi = \chi_0 + \frac{C}{T - \theta_W}$, see insets of Fig. 1. This implies that with increasing degree of dilution by Ti substitution the local moment behavior persists and the decrease of the Curie constant is compatible with the dilution of Ir moments by nonmagnetic Ti (see Ref. [24]). Small temperature independent van Vleck contributions (χ_0) are of order 10^{-5} cm³/mol. The AF Weiss temperature changes from -125 K at $x = 0$ to -18 K for $x = 0.26$ indicating a continuous decrease of the CW scale with magnetic depletion for the Na-system.

Field-cooled (FC) and zero-field cooled (ZFC) measurements at very low field of 5 mT shown in Fig. 1 display cusps for ZFC and a clear separation between FC and ZFC traces at low T, which are characteristic signatures for spin-glass (SG) behavior. The freezing temperature T_g has been determined from the maxima in ZFC traces, as indicated by vertical arrows in Fig. 1. For the lowest doping level ($x = 0.015$) in $Na_2(Ir_{1-x}Ti_x)O_3$, long-range magnetic ordering is still present below 15 K [24]. For higher doping, we find a reduction of $T_g = 6.8$ K for $x = 0.05$ to 2 K for $x = 0.26$. The SG behavior is also confirmed by frequency dependent ac susceptibility measurements for $x = 0.17$, which show a sharp cusp at T_g and a pronounced frequency dependence in the position of that cusp [24]. We have also measured the heat capacity (C) for this concentration and found a broad hump in C/T above T_g, which confirms the absence of long-range ordering and indicates SG freezing [24].

Next, we discuss the effect of nonmagnetic depletion for the Li system. As shown in Fig. 2, $Li_2(Ir_{1-x}Ti_x)O_3$ polycrystals display CW behavior between 100 and 300 K (cf. inset). Here, χ_0 ranges between -1×10^{-5} and -5×10^{-5} cm³/mol. Remarkably, the observed Weiss temperatures are very similar for all different investigated samples. For $x = 0.55$, we observe -25 K, which is close to -33 K for $x = 0$. Hence the CW scale remains almost unchanged for more than 50% dilution
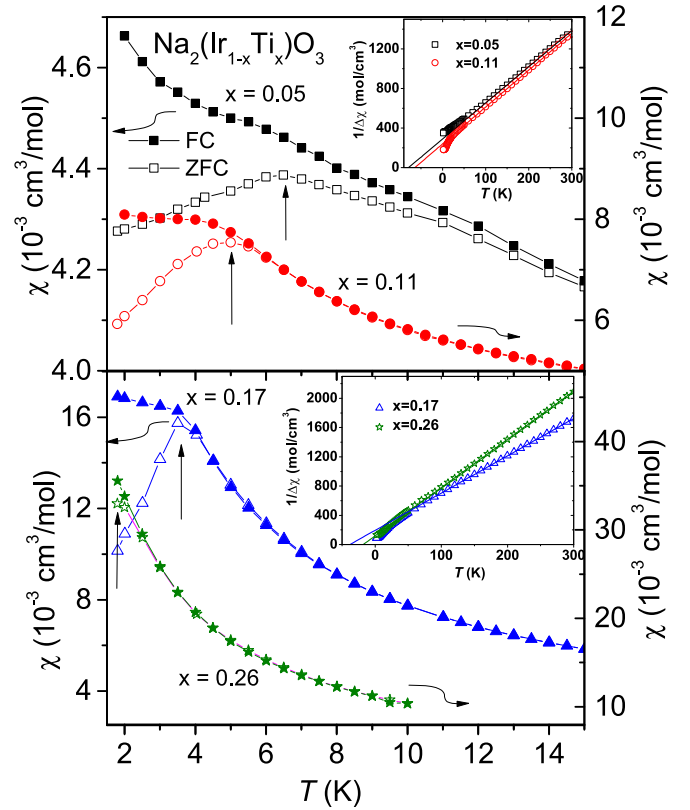

FIG. 1. (Color online) Field-cooled (FC) and zero-field-cooled (ZFC) susceptibility vs temperature as indicated by filled and open symbols, respectively, for $Na_2(Ir_{1-x}Ti_x)O_3$ with $x = 0.05, 0.11$ (top) and 0.17, 0.26 (bottom). Vertical arrows mark T_g. Respective insets display $1/\Delta\chi$ (with $\Delta\chi = \chi - \chi_0$) vs T. Solid lines indicate Curie-Weiss behavior.
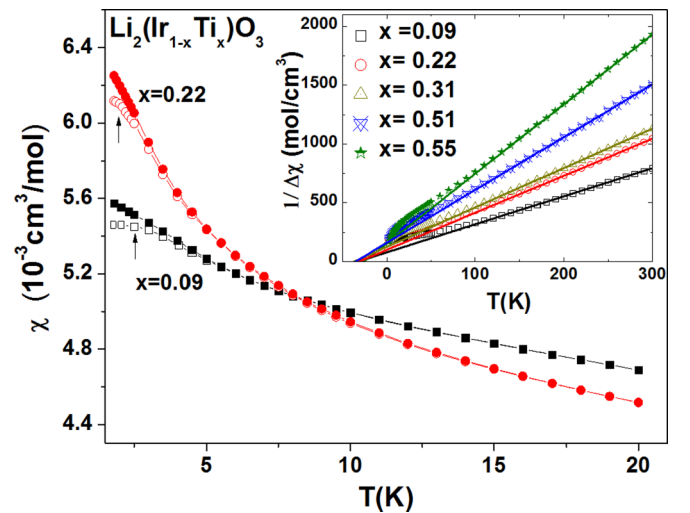

FIG. 2. (Color online) FC and ZFC susceptibility (represented by filled and open symbols, respectively) for $Li_2(Ir_{1-x}Ti_x)O_3$ with $x = 0.09$ and 0.22, measured at $H = 0.01$ T. Vertical arrows mark T_g. The inset displays $1/\Delta\chi$ vs T for all investigated x. Solid lines illustrate CW behavior.
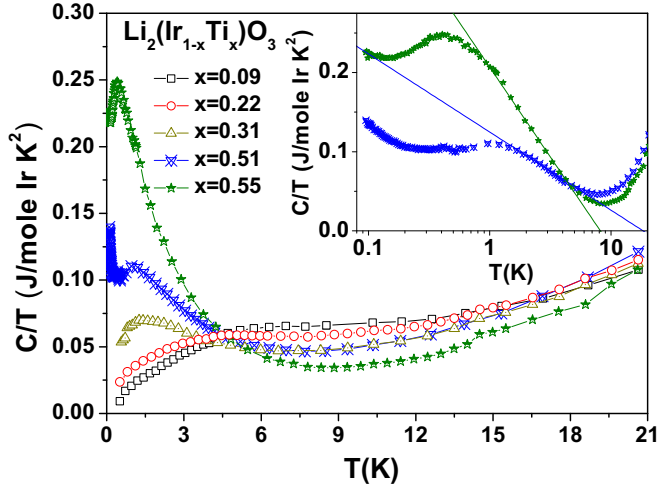
FIG. 3. (Color online) Specific heat as C/T vs T for various $Li_2(Ir_{1-x}Ti_x)O_3$ samples. The inset displays the low-T data for $x = 0.51$ and 0.55 on a $\ln(T)$ axis. Broad maxima indicate T_g, above which a logarithmic temperature dependence is found (see lines).

of magnetic moments in the Li system in stark contrast to its drastic reduction found for the Na system. At low temperatures, a hysteresis between FC and ZFC susceptibility data is found, similar as for the Na system. Figure 2 shows a separation between the FC and ZFC susceptibility, which confirms $T_g = 3.5$ and 2 K for $x = 0.09$ and 0.22, respectively (vertical arrows in Fig. 2 indicate T_g). The ac susceptibility also shows a strong frequency dependence for these two compositions. Similar SG freezing behavior is also present at higher doping below the temperature limit of our SQUID magnetometer (1.8 K) (see below).

We have measured for all $Li_2(Ir_{1-x}Ti_x)O_3$ samples the heat capacity down to 0.4 K and extended the data down to 50 mK for the two highest concentrations, see Fig. 3. For $x = 0.09$ and 0.22, we observe broad maxima in heat capacity divided by temperature C/T around $1.4T_g$, which is characteristic for SG transitions (see Fig. 3). For $x = 0.31, 0.51$, and 0.55, similar broad maxima are found at low temperatures. With increasing x, the position of these maxima shifts from 1.25 to 0.41 K for $x = 0.31$ to 0.55. The respective T_g values are determined by the position of the maximum divided by 1.4. From Fig. 3, it is unambiguously clear that even beyond 50% substitution of magnetic Ir sites by nonmagnetic Ti in the Li-honeycomb system, SG freezing persists and T_g continuously shifts to lower temperatures with increasing x. Strikingly, C/T for $x = 0.51$ and 0.55 does not approach 0 at lowest temperatures as expected for insulators but rather saturates (above a low-T nuclear upturn). This implies that a significant amount of magnetic entropy is shifted to low temperatures.

As indicated by the straight lines in the inset of Fig. 3, a logarithmic increase of C/T is found for $x = 0.51$ and 0.55 upon cooling from about 8 K down to the SG freezing. Such behavior is often found near magnetic instabilities and considered as signature of quantum criticality. We have also observed a strong nonmonotonic field dependence of C/T for $x = 0.51$ [24] and 0.55 (Fig. 4).
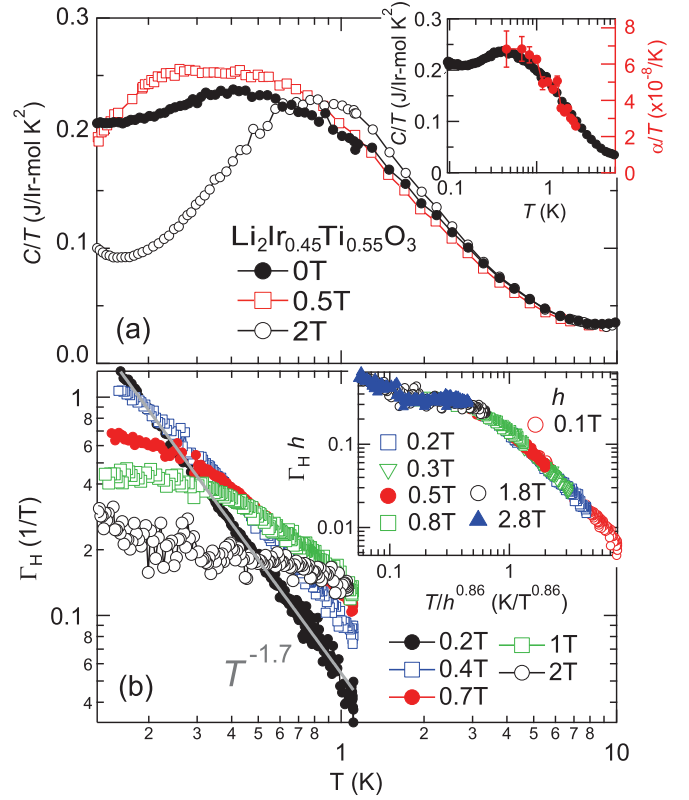

FIG. 4. (Color online) (Top) Specific heat as C/T vs T (on logarithmic scale) at various fields for $Li_2(Ir_{1-x}Ti_x)O_3$, $x = 0.55$. The inset displays zero field data together with respective thermal expansion data as α/T. (Bottom) Magnetic Grüneisen parameter $\Gamma_H = T^{-1}(dT/dH)_S$ at different magnetic fields vs T (on log-log scale). The solid line indicates the $T^{-1.7}$ divergence at 0.2 T. The inset displays scaling behavior $\Gamma_H h$ vs T/h^ϵ with $\epsilon = 0.86$ and $h = (H - 0.2 \text{ T})$.

The adiabatic magnetocaloric effect or magnetic Grüneisen parameter $\Gamma_H = T^{-1}(dT/dH)_S$ is a sensitive probe of quantum criticality and is expected to diverge as a function of temperature with a power-law function at the critical field H_c for a field-induced quantum critical point (QCP) [25]. Figure 4 displays the temperature dependence of Γ_H at different magnetic fields for $Li_2(Ir_{1-x}Ti_x)O_3$, $x = 0.55$. At a low field of 0.2 T, a divergence with exponent of -1.7 is found over at least one decade in T, indicating quantum critical behavior with a low critical field. At 0.4 T and larger fields, $\Gamma_H(T)$ saturates upon cooling and the saturation temperature increases with increasing field indicating that fields drive the system away from quantum criticality. The data at various different fields collapse on a single curve when plotted as $\Gamma_H h$ versus T/h^ϵ (see inset of lower panel of Fig. 4). Here, h denotes the difference in field from the critical field, i.e., $h = H - 0.2$ T and the scaling exponent amounts to $\epsilon = 0.86$. The critical field of 0.2 T is consistent with the power-law divergence of $\Gamma_H(T)$ only observed at 0.2 T. Furthermore, the nonmonotonic field dependence of the low-temperature specific heat is probably due to the small finite H_c. A similar divergence and scaling of the magnetic Grüneisen ratio is also found for the $x = 0.51$ sample [24].
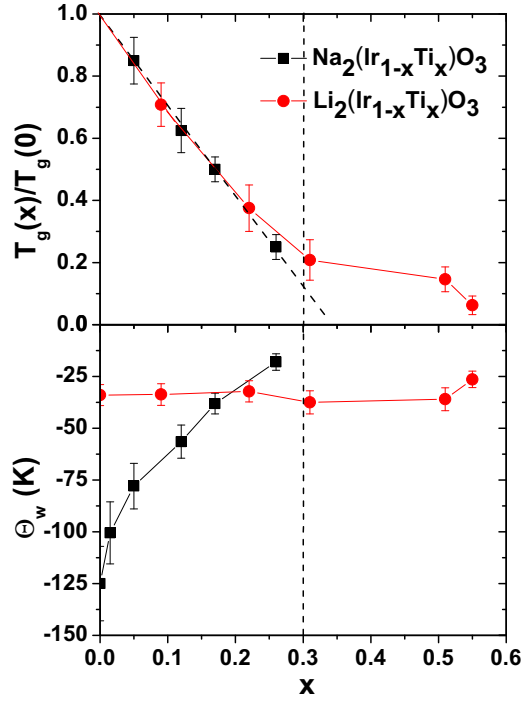
FIG. 5. (Color online) Evolution of normalized spin glass ordering temperatures (top) and Curie Weiss temperatures (bottom) for $Na_2(Ir_{1-x}Ti_x)O_3$ and $Li_2(Ir_{1-x}Ti_x)O_3$. The vertical dotted line at $x = 0.3$ indicates the percolation threshold in the honeycomb lattice. The dashed black line in the upper panel indicates the linear suppression of T_g for $Na_2(Ir_{1-x}Ti_x)O_3$.

Interestingly, for certain models, the possibility of simultaneous percolation and quantum criticality has been investigated theoretically [26–28].

To further characterize the low-temperature magnetic properties of depleted $Li_2(Ir_{1-x}Ti_x)O_3$, we have studied the temperature dependence of the linear thermal expansion coefficient $\alpha(T) = L^{-1}dL/dT$ (L: sample length) for $x = 0.55$, see upper inset of Fig. 4. The large values of order 10^{-6} K^{-1} around 1 K must originate from the magnetic properties (the phonon contribution is several orders of magnitude smaller). Interestingly, α/T perfectly scales with C/T indicating a temperature independent thermal Grüneisen ratio $\Gamma \sim \alpha/C$. This proves the absence of a QCP as function of pressure [25] and resembles the case of $CePd_{1-x}Rh_x$ where $\Gamma(T)$ also does not diverge due to the smeared quantum phase transition (QPT) [29]. The observed entropy accumulation at low T, which is quenched by a magnetic field but remains unaffected by pressure (or changes in composition) would then arise from weakly coupled magnetic clusters. Our

low-temperature experiments on $Li_2(Ir_{1-x}Ti_x)O_3$ thus prove that SG formation survives upon substantial magnetic depletion up to $x = 0.55$ leading to a smeared QPT.

The variation of the SG freezing temperatures for the depleted Na and Li systems is summarized in the upper panel of Fig. 5. In both systems, already small magnetic depletion induces a SG transition, highlighting the importance of magnetic frustration, and the freezing temperature T_g displays a linear suppression at low Ti concentration x. However, the evolution of the Weiss temperature shown in the lower panel indicates a substantially different response to magnetic depletion of the two systems. While for the Na-system a drastic reduction of $|\Theta_W|$ indicates a suppression of the average magnetic couplings by dilution, $|\Theta_W|$ remains unchanged in case of the Li-system. In addition, for the Li system the signatures of SG formation extend to large $x \sim 0.55$, where signatures of a smeared QPT are observed. Although we could not study $Na_2(Ir_{1-x}Ti_x)O_3$ at large x, the evolution of the magnetic coupling strength (from $|\Theta_W|$) suggests that the QPT for this system is located at significantly lower x. Recently, classical Monte Carlo simulations on depleted next-neighbor HK and J_1-J_2-J_3 Heisenberg models found that in the former case SG freezing disappears beyond the site percolation threshold $x_p = 0.3$, while in the latter case, with substantial further neighbor couplings it persists much beyond x_p [21]. Comparison with our data suggests that Na_2IrO_3 is governed dominantly by the nearest-neighbor HK model, whereas for the Li-system interactions beyond nearest neighbor are significantly important. Interestingly, $x = 0.50$ is the site percolation threshold for a triangular lattice and for J_2 exchange only, the honeycomb system corresponds to two decoupled triangular lattices. Thus the observed smeared QPT must be associated with further neighbor interactions. We also note, that recent theoretical work related to Li_2IrO_3 found that the low-Q spiral ordering in combination with the AF Weiss temperature $\Theta_W = -30$ K requires a model with second neighbor Kitaev and Heisenberg interactions [30].

To summarize, we have found differing behaviors in depleted honeycomb Na_2IrO_3 and Li_2IrO_3, which suggests the importance of substantial further neighbor magnetic interactions for Li_2IrO_3. In $Li_2(Ir_{1-x}Ti_x)O_3$ SG freezing persists to a regime at $x \sim 0.55$ for which indications of a smeared quantum phase transition is observed. Magnetism in this interesting regime could be further investigated by NMR, μSR or neutron scattering.

[1] D. Pesin and L. Balents, Nat. Phys. **6**, 376 (2010).

[2] S. J. Moon, H. Jin, K. W. Kim, W. S. Choi, Y. S. Lee, J. Yu, G. Cao, A. Sumi, H. Funakubo, C. Bernhard, and T. W. Noh, Phys. Rev. Lett. **101**, 226402 (2008).

[3] B. J. Kim, Hosub Jin, S. J. Moon, J.-Y. Kim, B.-G. Park, C. S. Leem, Jaejun Yu, T. W. Noh, C. Kim, S.-J. Oh, J.-H.

Park, V. Durairaj, G. Cao, and E. Rotenberg, Phys. Rev. Lett. **101**, 076402 (2008).

[4] B. J. Kim, H. Ohsumi, T. Komesu, S. Sakai, T. Morita, H. Takagi, and T. Arima, Science **323**, 1329 (2009).

[5] Y. Okamoto, M. Nohara, H. Aruga-Katori, and H. Takagi, Phys. Rev. Lett. **99**, 137207 (2007).

[6] J. Chaloupka, G. Jackeli, and G. Khaliullin, Phys. Rev. Lett. **105**, 027204 (2010).

[7] Choong H. Kim, Heung Sik Kim, Hogyun Jeong, Hosub Jin, and Jaejun Yu, Phys. Rev. Lett. **108**, 106401 (2012).

[8] Atsuo Shitade, Hosho Katsura, Jan Kunes, Xiao-Liang Qi, Shou-Cheng Zhang, and Naoto Nagaosa, Phys. Rev. Lett. **102**, 256403 (2009).

[9] Y. Singh and P. Gegenwart, Phys. Rev. B **82**, 064412 (2010).

[10] Y. Singh, S. Manni, J. Reuther, T. Berlijn, R. Thomale, W. Ku, S. Trebst, and P. Gegenwart, Phys. Rev. Lett. **108**, 127203 (2012).

[11] H. Gretarsson, J. P. Clancy, X. Liu, J. P. Hill, Emil Bozin, Yogesh Singh, S. Manni, P. Gegenwart, Jungho Kim, A. H. Said, D. Casa, T. Gog, M. H. Upton, Heung-Sik Kim, J. Yu, Vamshi M. Katukuri, L. Hozoi, Jeroen van den Brink, and Young-June Kim, Phys. Rev. Lett. **110**, 076402 (2013).

[12] I. I. Mazin, H. O. Jeschke, K. Foyevtsova, R. Valentí, and D. I. Khomskii, Phys. Rev. Lett. **109**, 197201 (2012).

[13] K. Foyevtsova, H. O. Jeschke, I. I. Mazin, D. I. Khomskii, and R. Valentí, Phys. Rev. B **88**, 035107 (2013).

[14] S. K. Choi, R. Coldea, A. N. Kolmogorov, T. Lancaster, I. I. Mazin, S. J. Blundell, P. G. Radaelli, Y. Singh, P. Gegenwart, K. R. Choi, S.-W. Cheong, P. J. Baker, C. Stock, and J. Taylor, Phys. Rev. Lett. **108**, 127204 (2012).

[15] J. Chaloupka, G. Jackeli, and G. Khaliullin, Phys. Rev. Lett. **110**, 097204 (2013).

[16] Youhei Yamaji, Yusuke Nomura, Moyuru Kurita, Ryotaro Arita, and Masatoshi Imada, arXiv:1402.1030.

[17] Li_2IrO_3 neutron scattering data presented in APS March meeting 2014 in Denver, Colorado, USA by S. K. Choi.

[18] S. Manni, Sungkyun Choi, I. I. Mazin, R. Coldea, Michaela Altmeyer, Harald O. Jeschke, Roser Valenti, and P. Gegenwart, Phys. Rev. B **89**, 245113 (2014).

[19] G. Cao, T. F. Qi, L. Li, J. Terzic, V. S. Cao, S. J. Yuan, M. Tovar, G. Murthy, and R. K. Kaul, Phys. Rev. B **88**, 220414(R) (2013).

[20] F. Trousselet, G. Khaliullin, and P. Horsch, Phys. Rev. B **84**, 054409 (2011).

[21] Eric C. Andrade and Matthias Vojta, arXiv:1309.2951.

[22] Tusharkanti Dey, A. V. Mahajan, P. Khuntia, M. Baenitz, B. Koteswararao, and F. C. Chou, Phys. Rev. B **86**, 140405(R) (2012).

[23] Y. Tokiwa and P. Gegenwart, Rev. Sci. Instr. **82**, 013905 (2011).

[24] See Supplemental Material at http://link.aps.org/supplemental/10.1103/PhysRevB.89.241102 on the structural parameter determination for $Li_2(Ir_{1-x}Ti_x)O_3$, magnetic properties of $Na_2(Ir_{1-x}Ti_x)O_3(x = 0.015)$, further χ_{ac} and $C(T)$ data on $Na_2(Ir_{1-x}Ti_x)O_3$ and Γ_H data for $Li_2(Ir_{1-x}Ti_x)O_3$.

[25] Lijun Zhu, Markus Garst, Achim Rosch, and Qimiao Si, Phys. Rev. Lett. **91**, 066404 (2003).

[26] Anders W. Sandvik, Phys. Rev. Lett. **89**, 177201 (2002).

[27] Rong Yu, Tommaso Roscilde, and Stephan Haas, Phys. Rev. Lett. **94**, 197204 (2005).

[28] Thomas Vojta and Jörg Schmalian, Phys. Rev. Lett. **95**, 237206 (2005).

[29] T. Westerkamp, M. Deppe, R. Küchler, M. Brando, C. Geibel, P. Gegenwart, A. P. Pikul, and F. Steglich, Phys. Rev. Lett. **102**, 206404 (2009).

[30] J. Reuther, R. Thomale, and S. Rachel, arXiv:1404.5818.